Proceedings of the 28th IEEE
EMBS Annual International Conference
New York City, USA, Aug 30-Sept 3, 2006

Power-Based Segmentation of Respiratory Signals Using Forward-Backward Bank Filtering

A. A. Aoude*,A. L. Motto*, H. L. Galiana*, K. A. Brown† and R. E. Kearney*
*Department of Biomedical Engineering, McGill University, Montreal, QC, Canada
†Department of Anaesthesia, McGill University Health Center/Montreal Children's Hospital, Montreal, QC, Canada

Abstract— **We present an automated method for the segmentation of ribcage and abdominal signals measured by noninvasive respiratory inductance plethysmography (RIP) into quiet breathing and artifact-corrupted segments. This procedure, which involves forward-backward filtering, is applicable to the automated off-line analysis of long records of respiratory signals. Examples of applications include home and sleep laboratory studies of cardiorespiratory data. The new procedure was successfully applied to the segmentation of cardiorespiratory signals acquired post-operatively from infants in the recovery room of the Montreal Children's Hospital (MCH).**

I. Introduction

SIGNAL processing procedures for marking the start and end times of "useful data segments" from a given record of respiratory and sleep data, or a subset thereof, have an important role in the diagnosis of clinically significant abnormalities. The term "useful data segment" is used here to designate any time interval of respiratory inductance plethysmography (RIP) signals that has a sufficiently high signal-to-noise ratio. A low signal-to-noise ratio arises when either or both ribcage and abdominal channels are corrupted by non-respiratory-induced movements, occurring, for example, when the subject is moving or being moved. For illustration, Fig. 3a provides a representative segment of an abdominal excursion signal measured by RIP in the recovery room of the Montreal Children's Hospital (MCH) [1]. The first 20-second period shows no apparent artifact whereas the following 11-second period is corrupted by artifact. This paper presents a signal processing procedure for the off-line, automated partitioning of RIP signals into segments either with or without artifacts.

The need for the automated segmentation of cardiorespiratory signals has been well recognized. Weese-Mayer *et al.* [2] reported that the performance of automated cardiorespiratory monitoring procedures could be significantly improved if signal segments corrupted with artifacts could be systematically identified. In [3], we proposed an automated procedure for estimating the phase relation between thoracic and abdominal excursions measured by noninvasive RIP. We noted that the performance of the phase estimator could be improved if it was combined with an automated procedure for partitioning a realization of RIP signals into periods with and without artifact corruption. Such automated signal segmentation procedures would also be useful in the analysis of long records of off-line respiration and sleep data. Furthermore, assuming that the probability of apnea occurring while a subject is moving or being moved is negligibly small, this procedure could be used to reject the hypothesis "apnea present", thereby improving the detection performance of automated apnea detectors.

In [4], we showed that a Neyman-Pearson energy-based detector could be used for the automated detection of artifacts. Reference [4] was mainly concerned with the on-line detection of artifacts whereas the present paper is concerned with the off-line detection and, therefore, uses forward-backward IIR (infinite impulse response) filters, producing an array of zero-phase filters with narrower pass bands and smaller transition bands. As a by-product, we obtain an estimate of the fundamental frequency of breathing up to a narrow band. The new method is aimed to be integrated into the cardio-respiratory monitor reported in [5].

II. Methods

We have developed a new method to allow for the automated segmentation of thoracic and abdominal signals into periods with artifact present and periods with artifact absent. From our previous study [3], it was observed that:

1) Quiet breathing signals are band limited with a given frequency.
2) The energy of sensor noise is negligible compared to quiet breathing components.
3) The energy of movement artifact is generally greater than that of quiet breathing and sensor noise with predominance at lower frequencies.

Using the above observations, we developed a method that uses a bank of IIR filters and average power to automatically segment respiratory data.

Fig. 1 shows a block diagram of the proposed method. Next, we describe the main components of the method.

A. High Pass Filter

To remove offsets and exponential decays observed in real infant data, a high pass filter with cut off frequency equal to 0.05Hz was used. As shown in Fig. 1, the original RIP signal is denoted $ab_1[n]$ and the high pass filtered signal is denoted $ab[n]$.

B. IIR Filter Bank

To estimate the fundamental frequency of the RIP signals, 13 filters were used to achieve little overlap between adjacent

1-4244-0033-3/06/$20.00 ©2006 IEEE.

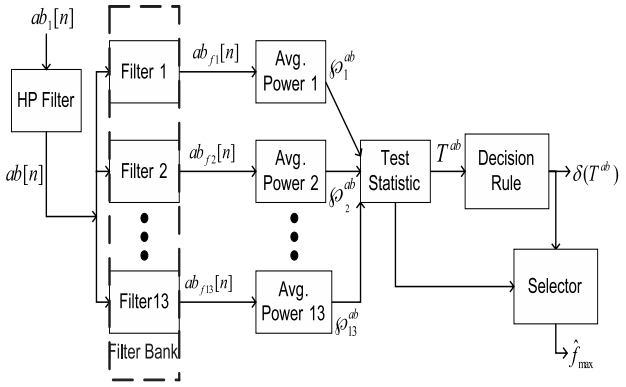

Fig. 1. Simplified diagram of proposed method for respiratory data segmentation. The figure depicts the process for the abdominal RIP signal ($ab_1[n]$). The same process is also applied to the ribcage RIP signal.

TABLE I

DESIGN SPECIFICATION OF IIR FILTERS[1]

Filter number (i)	f_l (Hz)	f_h (Hz)	n	ω_p (dB)	ω_s (dB)
1	0	0.2	7	0.01	50
2	0.15	0.35	3	0.1	30
3	0.3	0.5	4	0.01	40
4	0.45	0.65	4	0.01	40
5	0.6	0.8	4	0.01	50
6	0.75	0.95	4	0.01	50
7	0.9	1.1	4	0.01	50
8	1.05	1.25	4	0.01	50
9	1.2	1.4	4	0.01	50
10	1.35	1.55	4	0.01	50
11	1.5	1.7	4	0.01	50
12	1.65	1.85	4	0.01	50
13	1.8	2.0	4	0.01	50

[1] f_l denotes the filters' low cut off frequency; f_h denotes the filters' high cut off frequency; n denotes the filter order; ω_p denotes the maximum pass-band ripple level; ω_s denotes the minimum stop-band ripple attenuation level.

filter passband widths over [0, 2.0]Hz. The filters were chosen to span frequencies between 0 Hz and 2.0 Hz for two main reasons. Firstly, this range covers the range of fundamental frequencies of infant quiet breathing, as reported in [3]. Secondly, this range covers the low-frequency artifacts that are predominant in RIP signal corruption.

These filters were designed with a pass-band width of 0.2 Hz as well as specified pass-band and stop-band ripples (refer to Table I). Forward-backward filtering using IIR filters is used in the filter bank to perform zero-phase digital filtering and therefore not distort the phase between the thoracic and abdominal signals. The IIR filters were chosen to be elliptic or Cauer digital filters to obtain sharper roll offs and precise filter designs [6]. The optimal filter order was chosen using the elliptic low-pass filter order prediction formula described in [6, p.241] with the Signal Processing Toolbox of Matlab [7].

Table I enumerates the filters used and the specifications used to design them.

C. Average Power

The average power of the filtered RIP signals over a window length $2L+1$ was used to segment the signals. Let $\wp_i^{ab}[n,N]$ denote the average power value of the filtered abdominal signals over a window $N=2L+1$, then

$$\wp_i^{ab}[n,N]=\frac{1}{N}\sum_{k=n-L}^{n+L} ab_{fi}^2[k], \text{ for } i=1,2,...13 \qquad (1)$$

Where $ab_{fi}[n]$ represents the i^{th} filtered abdominal signal from the filter bank (refer to Fig. 1). Note that the ribcage power, $\wp_i^{rc}[n,N]$ is similarly defined.

D. Test Statistic

Since it is assumed that infant quiet breathing is between [0.4, 2]Hz and that artifacts are at lower frequencies, let $\mathcal{I}$ and $\mathcal{J}$ denote the index sets of the IIR bandpass filters covering the the quiet breathing and artifact frequency ranges, respectively; that is $\mathcal{I}=\{3,4,...,13\}$ and $\mathcal{J}=\{1,2\}$. Then, we can define the test statistic, T^{ab} as

$$T^{ab}[n]=\frac{\max\limits_i\{\wp_i^{ab}\}_{i\in\mathcal{I}}-\max\limits_j\{\wp_j^{ab}\}_{j\in\mathcal{J}}}{\max\limits_i\{\wp_i^{ab}\}_{i\in\mathcal{I}}+\max\limits_j\{\wp_j^{ab}\}_{j\in\mathcal{J}}}, \qquad (2)$$

where we use the convention $\frac{0}{0}=1$.

E. Decision Rule

The test statistic T^{ab} can then be used, together with a Neyman-Pearson threshold γ [8], for deciding

$$\delta(T^{ab})=\begin{cases}1, \text{if } T^{ab}\leq\gamma\\ 0, \text{if } T^{ab}>\gamma\end{cases} \qquad (3)$$

The decision rule above states that we choose the hypothesis $\mathcal{H}_0$ if $T^{ab}\leq\gamma$ and we choose the hypothesis $\mathcal{H}_1$ if $T^{ab}>\gamma$. Where the hypotheses are: $\mathcal{H}_0$: *Artifact Absent* and, $\mathcal{H}_1$: *Artifact Present*.

F. Selector

The selector in Fig. 1 yields an estimate of the breathing rate up to a narrow band, $\hat{f}_{max}$:

$$\hat{f}_{max}[n]=\delta[n]\min\{\arg\max_{i\in\mathcal{I}}\wp_i^{ab}[n]\}. \qquad (4)$$

Equation (4) states that $\hat{f}_{max}[n]=0$ if we decide *artifact present*; otherwise, $\hat{f}_{max}[n]$ is the index of a filter whose average power is maximum. The operation $\min$ ensures that $\hat{f}_{max}[n]$ is a singleton if more than one filter produces maximum average power.

III. APPLICATION TO SIMULATED DATA

A. Description of Simulated Data

The main concepts and derivations of the simulated breathing and additive noise signals used for this paper can be found in [3, pp.617-618]. In brief, these signals were composed of piecewise-linear frequency-modulated sinusoidal signals to model quiet breathing, white Gaussian noise to model sensor or electronic noises, and a stochastic diffusion process to model movement artifacts.

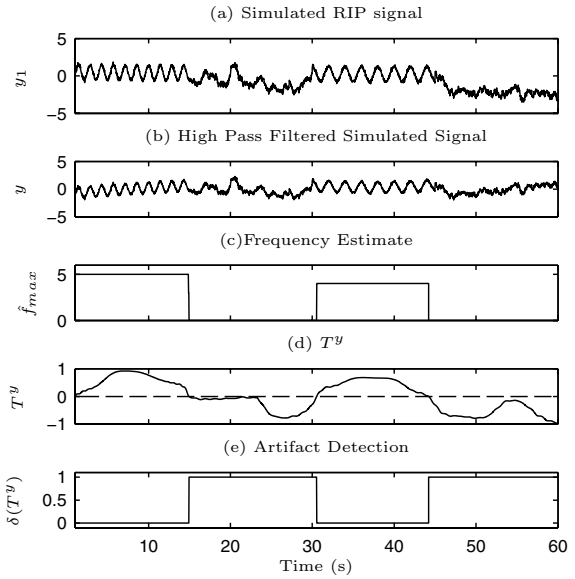

Fig. 2. Segmentation analysis of a 60s simulated segment of infant RIP signal. Note that for the simulated RIP signal a 0.7 Hz noise corrupted signal was used for the first 15s and a 0.5 Hz noise corrupted signal was used for time 30s to 45s. Time 15s to 30s and the last 15s of the simulated signal was predominantly composed of simulated movement artifact. (a) is the original signal, (b) is the high pass filtered signal, (c) is a plot of $\hat{f}_{max}$, (d) is a plot of the test statistic T^y (dashed line: $\gamma = 0$), and (e) is the decision $\delta(T^y)$. As expected, the method detect the artifact corrupted segments ($\delta(T^y) = 1$).

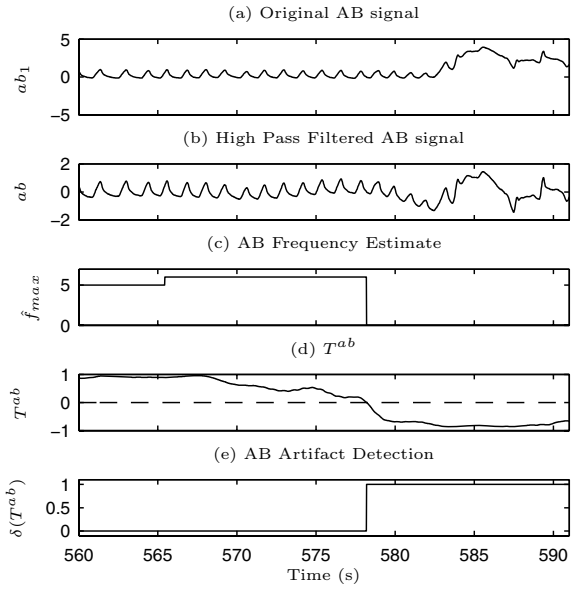

Fig. 3. Segmentation analysis of a 31s segment of abdominal ($ab_1[n]$) breathing excursions measured by inductance plethysmography of an infant (42 weeks old weighing 3.9 kg). Note that a quasi-sinusoidal breathing signal is observed for the first 20s followed by 11s of artifact corruption. (a) is the original RIP signal, (b) is the high pass filtered signal, (c) is a plot of $\hat{f}_{max}$, (d) is a plot of the test statistic T^{ab} (dashed line: $\gamma = 0$), and (e) is the decision $\delta(T^{ab})$. Note that for the time interval 577.5s to 582s the signal is composed of both, low frequency artifact and quiet breathing; since the power of the low frequency component is higher ($T^{ab} < 0$), the method labeled this segment as having artifact corruption.

B. Analysis of Simulated signals

To assess the effectiveness of our method, a simulated RIP signal was generated. This signal was composed of four segments. The first and third segments were normal breathing while, the second and fourth segments were predominantly composed of movement. All segments also had additive electronic noise.

Fig. 2 shows that our method correctly detects the artifact corrupted segments as well as the normal breathing segments in data with uncorrelated noise. In fact, the breathing segments are labeled with $\hat{f}_{max}$ values equal to 5 and 4 which are the expected values since they correspond to breathing frequencies anywhere in [0.6, 0.8]Hz and [0.45, 0.65]Hz respectively (the simulated frequencies were 0.7Hz and 0.5Hz respectively).

IV. Application to Infant Data

A. Description of Data

We now consider segmentation in breathing periods from 8 infants aged 44 ± 5 weeks, weighing 4.9 ± 1 kilograms. This data was previously reported by Brown *et al.* [1] as part of another study with appropriate ethics approval. This provided a convenient initial database for the validation of the proposed method. The observed continuous-time ribcage and abdominal signals (NIMS^{TM}, Respitrace Plus, North Bay Village, Florida), were amplified and filtered with 15Hz 8-pole Bessel filters (Frequency Devices, Haverhill, MA), and sampled at 50 Hz with a 12-bit analog-to-digital converter (Data Translation, Marlborough, MA). This data was stored on a computer using LABDAT^{TM} data acquisition software (RHT-InfoDat, Montreal). No attempt was made to calibrate the signals in absolute terms.

B. Analysis of Infants' Data

Since there does not exist a widely accepted and exact mathematical definition of normal breathing and artifact corrupted segments, the visual scoring of 8 infant data sets consisting of over 46 hours of data was considered. Thus, to asses the effectiveness of the method in segmenting the off-line data, the data acquired in [1] was visually scored by K. A. Brown (MD) in accordance to approved practice at the MCH. A comparison between the segmentation obtained using the automated method and the segmentation by visual scoring was used to determine the accuracy of the method.

1) Signal Segment Illustration: To illustrate the effectiveness of the method, Fig. 3 shows a segment of real infant data consisting of normal breathing followed by artifact corruption. As expected the artifact corrupted segment had $\delta(T^{ab})$ values (e) equal to 1, while the breathing segment had $\delta(T^{ab})$ values equal to 0.

Note that Fig. 2 and Fig. 3 were generated using the threshold $\gamma = 0$ for illustration purposes and using a window length (N) equal to 251 samples or 5s.

2) Comparison to Visual Scoring: Fig. 4 shows the distribution of T^{ab} over periods of quiet breathing and gross body movement for all 8 infant files in the data base used;

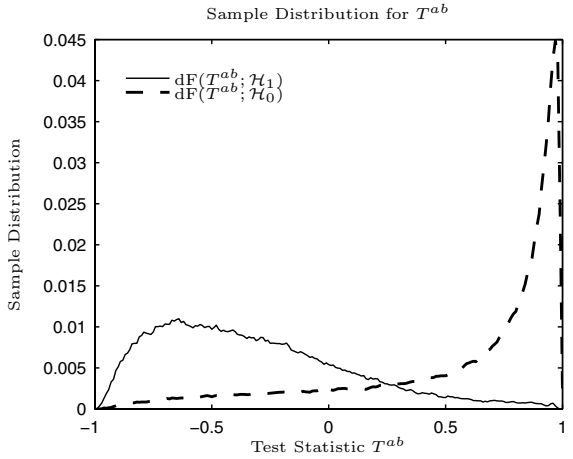

Fig. 4. Sample distributions of the test statistic T^{ab} for all 8 data files that have been visually scored by Dr. K. A. Brown. The plot shown was generated with N =251 (i.e. 5 seconds at 50 Hz), under the hypotheses $\mathcal{H}_0$ (movement artifact absent) and $\mathcal{H}_1$ (movement artifact present).

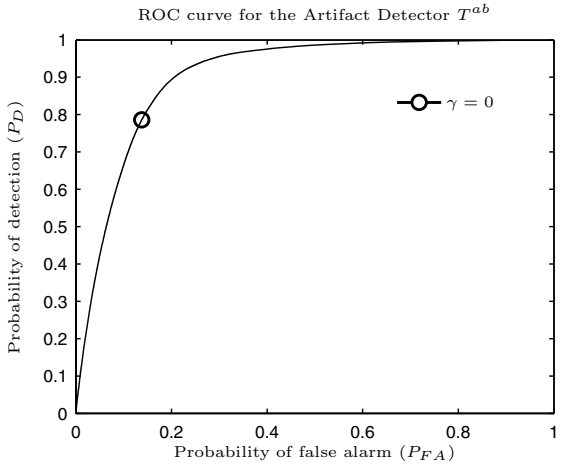

Fig. 5. Receiver operating characteristic for all 8 infants visually scored by Dr. K. A. Brown. The test statistic used was T^{ab} with N = 251 samples or 5 seconds. The circle indicates the probabilities for $\gamma = 0$.

that is under $\mathcal{H}_0$ and $\mathcal{H}_1$, respectively. We derived T^{ab} from the visual scoring done by K. A. Brown.

The performance of the proposed off-line detector, based on the visual scoring, is summarized in the receiver operating characteristic (ROC) for the test statistic T^{ab} of equation (2). The ROC plot is presented in Fig. 5, where P_{FA} denotes the probability of false alarm; that is, the probability of deciding *artifact present* when there is no artifacts and, where P_D denotes the probability of detection; that is, the probability of deciding *artifact present* when artifact is almost surely present.

Note that from the distribution shown in Fig. 4, P_D and P_{FA} for a given threshold γ can be found by solving

$$P_D = \int_{-1}^{\gamma} dF(T^{ab}, \mathcal{H}_1),\ P_{FA} = \int_{-1}^{\gamma} dF(T^{ab}, \mathcal{H}_0) \quad (5)$$

The segmentation presented above could be improved by further processing $\delta(T^{ab})$. This processing removes any detection segments that are smaller than 5s and, combines any two consecutive detection segments separated by a gap smaller than 5s. For example, using the threshold of γ equal 0, we obtained the following probabilities of detection and false alarm for all 8 infants, $P_D = 80\%$ and $P_{FA} = 15\%$. In comparison, after processing we obtained the following probabilities of detection and false alarm for all 8 infants, $P_D = 86\%$ and $P_{FA} = 11.25\%$. The results showed that it could prove useful to use T^{ab} as a decision criterion to segment real infant data.

V. Concluding Remarks

We have presented a new method to segment respiratory data into periods with or without movement artifact based on the frequency and energy content of RIP signals. The method is automated and used off-line to allow for segmentation of respiratory data. In addition, the method allows for repeatable analysis which is advantageous when compared to the inconsistencies of visual scoring.

Current studies are exploring the integration of the new procedure in the automated classification and detection of events such as obstructive and central apnea. The proposed procedure is fully automated and used off-line which will allow for less costly and more efficient analysis when compared to visual scoring.

Acknowledgment

This work was supported by a grant from the Natural Sciences and Engineering Research Council of Canada (NSERC).

References

[1] K. A. Brown, R. Platt, , and J. H. T. Bates, "Automated analysis of paradoxical ribcage motion during sleep in infants," *Pediatric Pulmonology*, vol. 33, pp. 38–46, 2002.

[2] D. E. Weese-Mayer, M. J. Corwin, M. R. Peucker, J. M. Di Fiore, D. R. Hufford, L. R. Tinsley, M. R. Neuman, R. J. Martin, L. J. Brooks, S. L. D. Ward, G. Lister, M. Willinger, and The CHIME Study Group, "Comparison of apnea identified by respiratory inductance plethysmography with that detected by end-tidal CO2 or thermistor," *American Journal of Respiratory and Critical Care Medicine*, vol. 162, pp. 471–480, 2000.

[3] A. L. Motto, H. L. Galiana, K. A. Brown, and R. E. Kearney, "Automated estimation of the phase between thoracic and abdominal respiratory movement signals," *IEEE Transactions on Biomedical Engineering*, vol. 52, no. 4, pp. 614–621, Apr. 2005.

[4] ——, "Detection of movement artifacts in respiratory inductance plethysmography: Performance analysis of a Neyman-Pearson energy-based detector," in *Proceedings of the 26th Annual International Conference of the IEEE Engineering in Medicine and Biology Society*, vol. 1, San Francisco, CA, Sep. 1–5 2004, pp. 49–52.

[5] S. S. Semienchuk, A. L. Motto, H. L. Galiana, K. A. Brown, and R. E. Kearney, "A portable, PC-based monitor for automated, on-line cardiorespiratory state classification," in *Proc. 27th Annual International Conference of the IEEE Engineering in Medicine and Biology Society*, Shangai, China, Sep. 1–4, 2005.

[6] L. R. Rabiner and B. Gold, *Theory and Application of Digital Signal Processing*. Englewood Cliffs, NJ: Prentice-Hall, 1975.

[7] The MathWorks. (2004, Jun.) Signal processing toolbox user's guide. [Online]. Available: http://www.mathworks.com/access/helpdesk/help/toolbox/signal/

[8] S. M. Kay, *Fundamentals of Statistical Signal Processing—Volume II: Detection Theory*. Englewood Cliffs, NJ: Prentice-Hall, 1998.